European Radiology (2019) 29:1518–1526
https://doi.org/10.1007/s00330-018-5715-5

ULTRASOUND

Development and validation of an ultrasound-based nomogram to improve the diagnostic accuracy for malignant thyroid nodules

Bao-liang Guo [1] · Fu-sheng Ouyang [1] · Li-zhu Ouyang [2] · Zi-wei Liu [1] · Shao-jia Lin [1] · Wei Meng [1] · Xi-yi Huang [3] · Hai-xiong Chen [1] · Shao-ming Yang [1] · Qiu-gen Hu [1]

Received: 3 April 2018 / Revised: 17 July 2018 / Accepted: 14 August 2018 / Published online: 12 September 2018

Abstract

Objectives The aim of this study was to develop an ultrasound-based nomogram to improve the diagnostic accuracy of the identification of malignant thyroid nodules.

Methods A total of 1675 histologically proven thyroid nodules (1169 benign, 506 malignant) were included in this study. The nodules were grouped into the training dataset (n = 700), internal validation dataset (n = 479), or external validation dataset (n = 496). The grayscale ultrasound features included the nodule size, shape, aspect ratio, echogenicity, margins, and calcification pattern. We applied least absolute shrinkage and selection operator (lasso) regression to select the strongest features for the nomogram. Nomogram discrimination (area under the receiver operating characteristic curve, AUC) and calibration were assessed. The nomogram was subjected to bootstrapping validation (1000 bootstrap resamples) to calculate a mean AUC and 95% confidence interval (CI).

Results The nomogram showed good discrimination in the training dataset, with an AUC of 0.936 (95% CI: 0.918–0.953) and good calibration. Application of the nomogram to the internal validation dataset also resulted in good discrimination (AUC: 0.935; 95% CI, 0.915–0.954) and good calibration. The model tested in an external validation dataset demonstrated a lower AUC of 0.782 (95% CI: 0.776–0.789).

Conclusions This ultrasound-based nomogram can be used to quantify the probability of malignant thyroid nodules.

Key Points

- *Ultrasound examination is helpful in the differential diagnosis of malignant and benign thyroid nodules.*
- *However, ultrasound accuracy relies heavily on examiner experience.*
- *A less subjective diagnostic model is desired, and the developed nomogram for thyroid nodules showed good discrimination and good calibration.*

Keywords Thyroid nodule · Ultrasonography · Diagnosis · Nomogram · Area Under Curve

Baoliang Guo and Fusheng Ouyang contributed equally to this work.

✉ Qiu-gen Hu
qiugenhu@126.com

[1] Department of Radiology, Shunde Hospital of Southern Medical University (The First People's Hospital of Shunde), No.1, Penglai Road, Daliang District, Shunde, Foshan, Guangdong, People's Republic of China

[2] Department of Ultrasound, Shunde Hospital of Southern Medical University (The First People's Hospital of Shunde), Foshan, Guangdong, People's Republic of China

[3] Department of Laboratory, Lecong Hospital of Shunde, Foshan, Guangdong, People's Republic of China

Abbreviations

AUC	Area under the curve
CI	Confidence interval
FNA	Fine-needle aspiration
Lasso	Least absolute shrinkage and selection operator
SD	Standard deviation

Introduction

The incidences of thyroid nodules and thyroid cancer are increasing worldwide, largely due to enhanced diagnostic practices [1]. With the application of ultrasound technology to thyroid scans, the number of thyroid nodules found using non-palpation methods has increased rapidly, to 20–67% in the general population [2]. China has the largest population in the world, and the burden of clinical management of thyroid nodules and thyroid cancer is enormous [3]. A recent large, community-based study revealed that the prevalence of thyroid nodules in Chinese adults on conventional ultrasound examination was 49%. Nevertheless, only a small percentage (approximately 5–10%) of thyroid nodules were found to be malignant [4, 5]. Thus, it is critical to differentiate malignant from benign thyroid nodules to avoid unnecessary fine needle aspiration (FNA) biopsy and overtreatment such as surgery.

There are currently several methods available to detect and evaluate thyroid nodules, including ultrasound, computed tomography (CT), magnetic resonance imaging (MRI), radionuclide scan, positron emission tomography, and genetic testing [6–10]. Of these, conventional operator-dependent ultrasound is the most commonly used method, as it is non-invasive, convenient, economical, and non-radioactive [10]. The characteristics of malignant nodules on conventional ultrasound imaging include, but are not limited to, the presence of micro-calcification, hypoechogenicity, disorganized margins, and a taller-than-wide shape [3, 11]. However, these features have varying sensitivities and specificities for the diagnosis of malignant thyroid nodules. The complex structure of nodules results in complex ultrasound images and some confusion between benign and malignant nodules. Conventional operator-dependent ultrasound cannot satisfactorily distinguish between malignant and benign thyroid nodules. This practice can be improved with the use of machine learning methods. By "learning" from available data, these computational methods or models can automatically select the strongest predictors for clinical outcomes and improve the prediction process [12]. Nomograms are statistical predictive models that can be used to calculate the probability of a clinical outcome in an objective way [13]. In recent times, more doctors have started using nomograms to evaluate individual risks [14, 15].

Therefore, the purposes of this study were to identify the ultrasound features most associated with malignancy with the help of a machine learning method and to develop an ultrasound-based nomogram for the diagnosis of malignant thyroid nodules.

Materials and Methods

Patients and thyroid nodules

Ethical approval was obtained for this retrospective analysis, and the requirement for informed consent was waived. The training and internal validation datasets comprised an evaluation of the medical database from our department to identify patients diagnosed with confirmed benign or malignant thyroid nodules between January 2011 and November 2016. The external validation dataset comprised of cases from another hospital that underwent imaging between January 2015 and February 2017. The inclusion criteria of nodules were as follows: 1) the nodule was analyzed according to surgical histology within 1 month after examination, 2) the size of the nodule was ≤ 2.5 cm in its widest diameter and 3) the nodule had not been previously surgically treated. The exclusion criteria were: 1) inadequate cytologic results and no surgical histology, 2) indeterminate cytologic results and no surgical histology, 3) the nodule was diagnosed as "suspicious for papillary thyroid carcinoma" only on cytologic examination, and did not undergo surgical histology, and 4) duplicate nodules, defined as those sharing the same features by ultrasound, were removed from the dataset to satisfy the requirements for machine learning that all observations be independent of one another.

Conventional grayscale ultrasound imaging characteristics

We used Acuson Sequoia 512 (Siemens Healthineer) and 128XP sonographic scanners (Siemens Healthineers) equipped with 10–12 MHz linear probes for conventional ultrasound measurement. In the externally validated hospital, LOGIQ S7 and S8 (GE Healthcare's reporting and image management solution, ViewPoint* 6) equipped with 6–15 MHz linear probes were used. All patients were examined in the supine position with their necks extended with a pillow under the shoulders for better exposure of the lower thyroid margins. Scans of both thyroid lobes and isthmus were obtained in both transverse and longitudinal planes. Longitudinal and transverse images of the thyroid were obtained according to the American College of Radiology accreditation standards, and images were recorded on PACS workstations (GE Centricity; GE Healthcare). The grayscale ultrasound imaging characteristics of each nodule were retrospectively reviewed by two independent radiologists with more than 10 years of experience in thyroid imaging, and who were blinded to the clinical outcome. The imaging characteristics of each nodule included the size, shape, aspect ratio (height divided by width on transverse views, A/T), echogenicity, margins, and calcification pattern. Nodule size was classified according to the maximum diameter (D), as follows: D ≤ 0.5 cm, 0.5 < D ≤ 1.0 cm, 1.0 < D ≤ 1.5 cm, 1.5 < D ≤ 2.0 cm, or 2.0 < D ≤ 2.5 cm. Shape was classified as regular or irregular. The A/T was classified as < 1 or ≥ 1. The echogenicity was categorized as hyper-, iso-, hypo-echogenicity or absence. Margins were classified as well-defined or ill-defined and the calcification pattern was categorized as non-calcification, micro-calcification, macro-calcification, or both.

Selection of ultrasound imaging features

We used the least absolute shrinkage and selection operator (lasso) method to select the most significant features, and then built a logistic regression model that included the selected variables. All variables entered into the model were set as dummy variables. For the binary logistic regression model, the negative log-likelihood subjects to the sum of the absolute value of the coefficients is less than the tuning parameter λ. If λ is large, there is no effect on the estimated regression parameters, but as λ decreases, some coefficients may decrease to zero [16, 17]. We then selected λ with the smallest cross-validation error. Finally, the model was re-fit using all the observations and the selected λ. Most of the coefficients were reduced to zero, and the remaining non-zero coefficients were selected by lasso.

Development and validation of an individualized diagnostic nomogram

Nomograms are statistical models that are ideally suited for individualizing risk assessment. To provide the radiologists with a quantitative tool to diagnose the individual probability of malignant thyroid nodules, we built the diagnostic nomogram using the independent predictors selected by lasso to generate a combined indicator for estimating the probability of malignant thyroid nodule. The nomogram created in the training dataset was applied to the internal and external validation dataset, and the total point for each nodule were calculated. The nomogram was performed using the total points as a factor. The area under the receiver operating characteristic curve (AUC) was measured to quantify the discrimination of the nomogram. The nomogram was subjected to bootstrapping validation (1000 bootstrap resamples) to calculate a relatively robust AUC. Calibration curves were plotted to assess the calibration of the diagnostic nomogram, which was assessed by plotting the predicted versus the actual probability for quintiles of the predicted probability of malignancy within a nodule.

Statistical analysis

The inter- and intra-operator agreement were estimated by Cohen's Kappa. The grayscale features between benign and malignant thyroid nodules were compared using the Chi-square or Fisher's exact test. We reported the classification performance of logistic regression with the lasso using the training, internal validation and external validation datasets. The performance of the classification method relied heavily on the tuning of parameter λ, and thus a 10-fold cross-validation was applied to select λ using the minimum criteria.

The path of the AUC was also reported since the best performance could be obtained by selecting imaging features most associated with the malignancy. We developed a diagnostic nomogram in the training dataset based on the selected US features and tested it in the internal and external validation datasets. Nomogram discrimination and calibration were assessed. We repeated this process 1000 times to obtain the mean AUC and 95% CI of the models. All statistical analyses were performed using R version 3.2.3 (R Foundation for Statistical Computing).

Results

Basic characteristics of patients and nodules

There were 1675 thyroid nodules (training dataset n = 700, internal validation dataset n = 479, external validation dataset, n = 496) in 1498 patients, including 1169 (69.8%) benign and 506 (30.2%) malignant nodules. Among the patients, 521 were men and 977 were women with a mean age (± standard deviation) of the patients of 44.1 ± 13.2 years (range: 18–85 years). Features of these nodules in grayscale ultrasound are summarized in Table 1. There were significant differences in shape, aspect ratio, echogenicity, margin and calcification pattern between benign and malignant thyroid nodules (all $p < 0.001$). However, there was no difference in size between benign and malignant thyroid nodules ($p = 0.825$–0.986).

The intra-operator and inter-operator agreement

Intra- or inter-operator agreement of grayscale ultrasound features were between 0.76 and 0.98 (Table 2).

Feature selection

Ultrasound imaging features such as shape, aspect ratio, echogenicity, margin, and calcification pattern had non-zero coefficients when the lasso logistic regression model was selected (Fig. 1a and b).

Diagnostic performance of the nomogram in the training dataset

The nomogram that incorporated all five important diagnostic factors was developed and presented. The mean AUC for the nomogram was 0.936 (95% CI, 0.918–0.953) for the training dataset (Fig. 2). The calibration curve of the nomogram for the probability of malignant thyroid nodules showed good agreement between prediction and observation in the training dataset (Fig. 3a).

Validation of the diagnostic nomogram

Application of the developed nomogram in the internal validation dataset still yielded good discrimination (AUC, 0.935; 95% CI, 0.915–0.954). Good calibration was observed for the probability of a malignancy in the internal validation group (Fig. 3b). Good calibration was also observed for the probability of malignancy in the external validation (Fig. 3c). The externally

Table 1 Comparison of grayscale ultrasound features of benign and malignant thyroid nodules in the training, internal validation, and external validation datasets

Features	Training dataset			Internal validation dataset			External validation dataset		
	Benign (n = 448)	Malignant (n = 252)	*p* value*	Benign (n = 373)	Malignant (n = 106)	*p* value	Benign (n = 348)	Malignant (n = 148)	*p* value*
Size (cm)									
≤ 0.5	4 (0.9)	3 (1.2)	0.928[a]	3 (0.8)	2 (1.9)	0.924[a]	3 (0.9)	1 (0.8)	0.997[a]
0.5–1.0	38 (8.5)	26 (10.3)		46 (12.3)	14 (13.2)		31 (8.9)	14 (9.5)	
1.0–1.5	214 (47.8)	116 (46.0)		176 (47.2)	49 (46.2)		176 (50.6)	75 (50.7)	
1.5–2.0	119 (26.6)	65 (25.8)		99 (26.5)	27 (25.5)		100 (28.7)	43 (29.1)	
2.0–2.5	73 (16.3)	42 (16.7)		49 (13.1)	14 (13.2)		38 (10.9)	15 (10.1)	
Echogenicity									
Absence	1 (0.2)	25 (9.9)	< 0.001[a]	1 (0.3)	20 (18.9)	< 0.001[a]	2 (0.6)	18 (12.2)	< 0.001[a]
Isoechoicity	106 (23.7)	185 (73.4)		85 (22.8)	65 (61.3)		81 (23.3)	88 (59.5)	
Hypoechoicity	330 (73.7)	40 (15.9)		279 (74.8)	18 (17.0)		259 (74.4)	34 (23.0)	
Hyperechoicity	11 (2.5)	2 (0.8)		8 (2.1)	3 (2.8)		6 (1.7)	8 (5.4)	
Margins									
Well-defined	366 (81.7)	52 (20.6)	< 0.001	306 (82.0)	36 (34.0)	< 0.001	289 (83.0)	45 (30.4)	< 0.001
Ill-defined	82 (18.3)	200 (79.4)		67 (18.0)	70 (66.0)		59 (17.0)	103 (69.6)	
Shape									
Regular	366 (81.7)	44 (17.5)	< 0.001	306 (82.0)	23 (21.7)	< 0.001	252 (92.0)	42 (28.4)	< 0.001
Irregular	82 (18.3)	208 (82.5)		67 (18.0)	83 (78.3)		22 (8.0)	106 (71.6)	
Aspect ratio (A/T)									
≤ 1	424 (94.6)	141(56.0)	< 0.001	350 (93.8)	50 (47.2)	< 0.001	322 (92.5)	109 (73.6)	< 0.001
> 1	24 (5.4)	111 (44.0)		23 (6.2)	56 (52.8)		26 (7.5)	39 (26.4)	
Calcification pattern									
Non-	336 (75.0)	49 (19.4)	< 0.001	275 (73.7)	32 (30.2)	< 0.001	262 (75.3)	32 (21.6)	< 0.001
Micro-	24 (5.4)	180 (71.4)		22 (5.9)	56 (52.8)		24 (6.9)	94 (63.5)	
Macro-	54 (12.1)	7 (2.8)		46 (12.3)	9 (8.5)		40 (11.5)	15 (10.1)	
Micro+macro	34 (7.6)	16 (6.3)		30 (8.0)	9 (8.5)		22 (6.3)	7 (4.7)	

Unless otherwise indicated, data are numbers of nodules, and numbers in parentheses are percentages

*p values were calculated by using generalized estimating equation analysis

[a] Fisher's exact test

Table 2 Intra- and inter-operator grayscale ultrasound feature measurement reliability: Kappa coefficient

	Intra-operator		Inter-operator	
Features	Operator 1	Operator 2	Measurement 1	Measurement 2
Size	0.91		0.95	
Echogenicity	0.79		0.82	
Margins	0.76		0.81	
Shape	0.78		0.83	
Aspect ratio	0.92		0.98	
Calcification pattern	0.82		0.87	

validated nomogram yielded a lower AUC of 0.782 (95% CI, 0.776–0.789) for the probability of malignancy.

An example of the nomogram in use

For example, the risk of malignancy in patient 1, who has a nodule with ill-defined margins, irregular shape, aspect ratio > 1, hypoechogenicity, and microcalcification (Fig. 4a), could be calculated to be more than 99% (Fig. 4b). Pathology proves it is a papillary thyroid carcinoma (Fig. 4c, h & e, ×40). Patient 2, who has a nodule with well-defined margins, regular shape, aspect ratio <1, isoechogenicity, and no calcifications (Fig. 4d), has a risk of less than 10% (Fig. 4e). Pathology confirms it is a nodular goiter (Fig. 4f, h & e, ×40).

Discussion

We developed and validated an ultrasound-based nomogram to improve the diagnosis of malignant thyroid nodules (≤ 2.5 cm in diameter). The nomogram incorporated five factors of the conventional ultrasound imaging characteristics of nodules: shape, echogenicity, margins, aspect ratio, and calcification pattern. We observed that the nomogram was highly discriminating in both the training dataset and the internal validation dataset. For external validation, the nomogram demonstrated a lower AUC. We developed an easy-to-use, repeated, and economical nomogram that facilitated the individualized prediction of malignant thyroid nodules.

Fine needle aspiration (FNA) has been widely accepted as the preferred detection technique for the assessment of non-toxic thyroid nodules. It is employed primarily in triage to identify those requiring surgery and to select the appropriate surgical procedures [18]. However, thyroid FNA has its limitations, due primarily to uncertain cytological features in the differentiation of benign and malignant follicular neoplasms, Hurthle cells, hyperplastic nodules, and follicular variants of papillary cancer [19, 20]. At best, thyroid FNA results are non-diagnostic, suspicious, or unclear in 20–30% of cases, and the risk of cancer varies from 5–75.5% in these groups

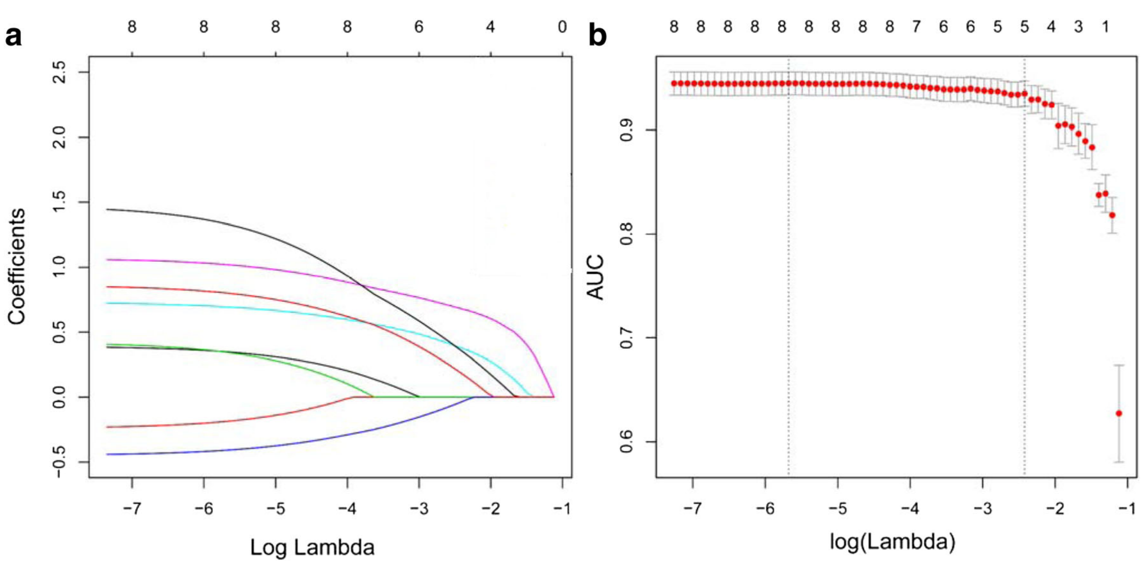

Fig. 1 Ultrasound imaging feature selection using the least absolute shrinkage and selection operator (lasso) logistic regression model. **a** Identification of the optimal penalization coefficient lambda (λ) in the lasso model used 10-fold cross-validation and the minimum criterion. As a result, a λ value of 0.067, with log (λ) = -2.71, was selected. **b** lasso coefficient profiles of the eight features. The dotted vertical line was plotted at the value selected using 10-fold cross-validation in Fig. 1a, for which the optimal λ resulted in five non-zero coefficients

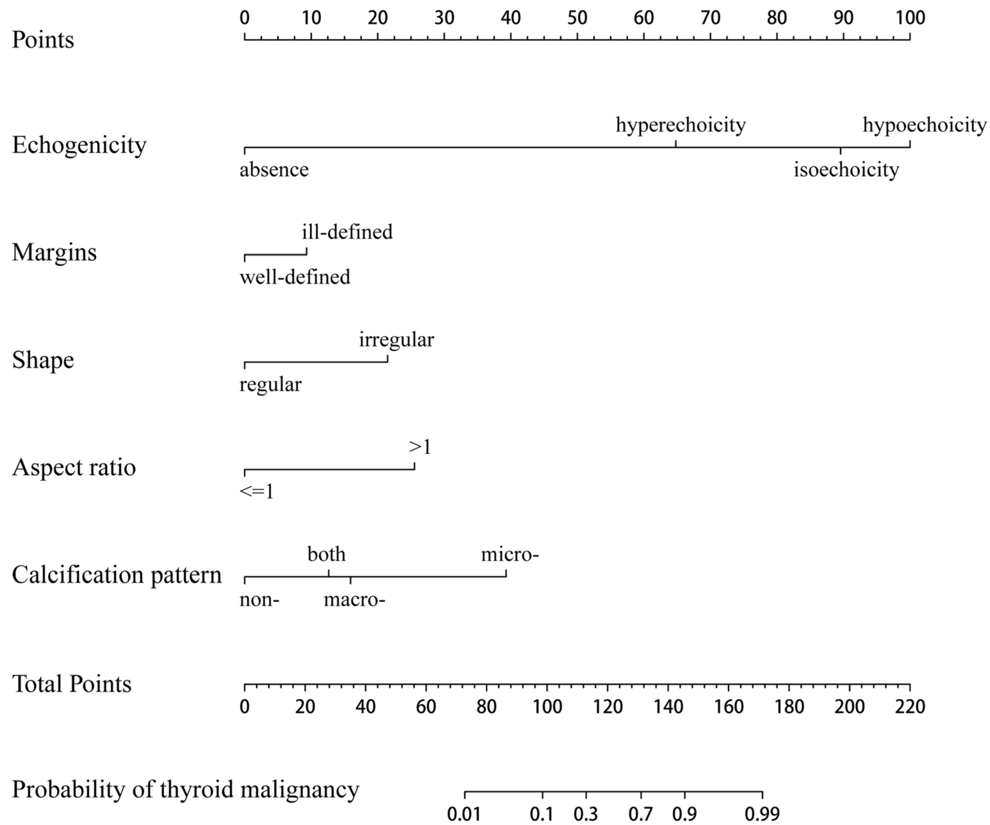

Fig. 2 Diagnostic nomogram. The nomogram was developed in the training dataset, with the size, shape, aspect ratio, margins, echogenicity, and calcification incorporated. The nomogram plot is provided for the variables selected and it provides a visible way to quickly obtain the individual prediction risk for the potential patient

[19]. At present, very limited clinical features (such as age and sex) can be considered in the diagnosis of malignant nodules. Therefore, there is a general consensus that FNA combined with ultrasound imaging is the preferred method to distinguish between benign and malignant thyroid nodules.

Conventional ultrasound has become the preferred imaging method for the diagnosis of thyroid nodules, but the diagnostic accuracy is influenced by the operator's experience. Some previous studies have evaluated the usefulness of the strain ratio, strain elastography, acoustic radiation force impulse imaging, and contrast-enhanced ultrasound to predict malignant nodules [21–24]. However, the usefulness of these methods remains controversial and is unconfirmed.

We aimed to develop and validate a less subjective model to enhance the operator's diagnostic performance, especially for operators with low proficiency. This study was conducted to identify the strongest predictors of malignant thyroid nodules with respect to the following factors: echogenicity,

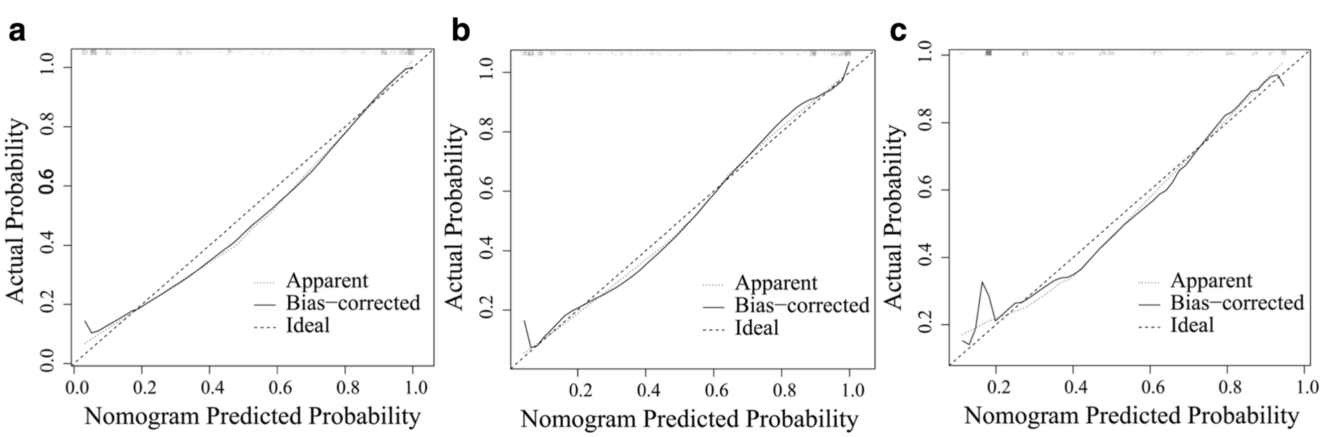

Fig. 3 The calibration curves of the nomogram in the training dataset (**a**), internal validation dataset (**b**) and external validation dataset (**c**) are reported. The x-axis is the nomogram predicted probability and the y-axis is the actual probability. The prediction performance can be measured by the difference of the fitted curve and slope 1 line (diagonal 45-degree line). The diagonal dotted line represents a perfect prediction by an ideal model. The solid line represents the performance of the nomogram, of which a closer fit to the diagonal dotted line represents a better prediction

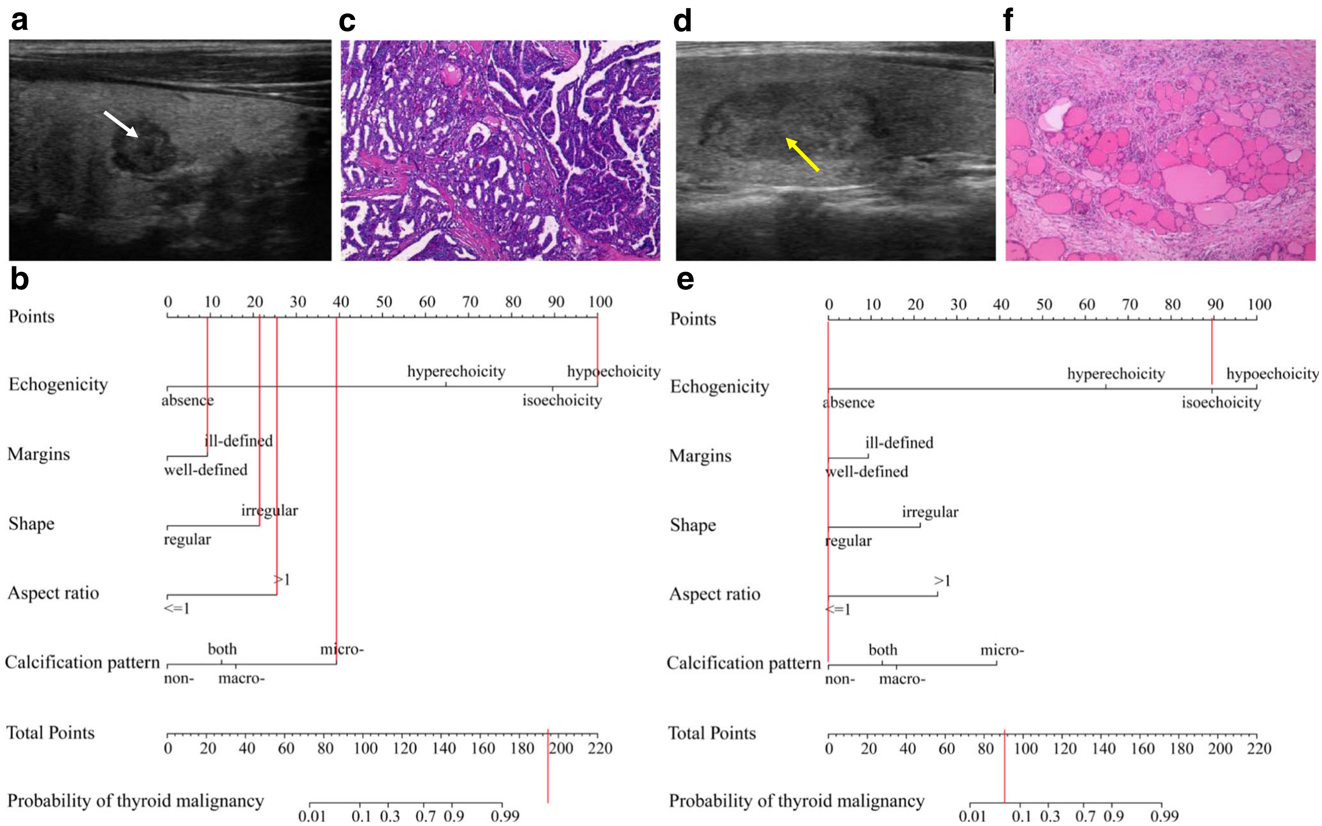

Fig. 4 Example of the nomogram in use. (**a**) shows a nodule (white arrow) with ill-defined margins, irregular shape, aspect ratio > 1, hypoechogenicity and microcalcification in patient 1, the risk of malignancy calculated by nomogram was more than 99% (**b**). Representative pathological image confirms a papillary thyroid carcinoma (**c**, × 40). (**d**) shows a nodule (yellow arrow) with well-defined margins, regular shape, aspect ratio <1, isoechogenicity and no calcification in patient 2, has a risk of less than 10% (**e**). Pathological image demonstrates a nodular goiter (**f** × 40)

contour, shape, aspect ratio, and calcification. It is recommended that ultrasound characteristics, rather than nodule size, be used to differentiate nodules, suggesting that thyroid nodules of any size should be further examined for malignancy [25]. Nodule size was not selected by lasso in our study, which was consistent with previous studies. In most cancer patients, the cluster contains a single nodule rather than multiple nodules. Most nodules in our study were single. No significant relationships were found between the number of nodules and malignancy [26]. It is accepted by most researchers that higher numbers of nodules do not increase the risk of malignancy [27]. Some previous studies compared the ultrasound and FNA results of thyroid nodules to the ultrasound criteria for the diagnosis of malignancy, including micro-calcification, hypo-echogenicity, taller-than-wide shape, and poorly defined margins [28, 29]. Consistent with previous studies, the features selected by lasso were deemed reliable. On the other hand, contrary to the method used in previous studies, we used a machine-learning algorithm to build a diagnostic model. Machine learning can be broadly defined as a computational method/model that uses experience (data) to improve performance or make accurate predictions [15]. These programmable computational methods are capable of "learning" from data and thus can automate and improve the prediction process. This easy-to-use and effective model only requires operators to report common ultrasound imaging characteristics. If cervical lymph node metastasis of a thyroid nodule occurs, the nodule will be diagnosed as malignant. The diagnosis of approximately 70% of nodules without cervical lymph node metastasis largely depends on this nomogram.

Despite the strong results, our study had several limitations. First, we did not analyze additional ultrasound characteristics, such as composition and number of nodules, because they showed no significant prediction value according to reports from many previous studies. Secondly, we could not identify the encapsulated follicular variant of papillary thyroid carcinoma from malignant thyroid nodules by ultrasound, though it has an excellent prognosis (and thus is termed a non-invasive follicular thyroid neoplasm with papillary-like nuclear features) [30]. In addition, because it had been newly reported, our pathology department had not differentiated it from malignant nodules. Lastly, our nomogram possibly had some inherent diagnostic errors (type I and type II errors) or not. For example, on the one hand, the diagnostic performance of our model depends on the accuracy of operator-reported imaging features, which explains why the AUC of the external validation improved to a smaller degree compared to that of the internal validation. On the other hand, the diagnostic performance of our model in thyroid nodules with inconclusive due to unclear or inadequate cytologic results. We intend to investigate this further in the future.

In conclusion, the present study developed and validated an ultrasound-based machine learning model to improve the diagnostic accuracy of the identification of malignant thyroid nodules. The model can be improved by the operator's experience and the addition of more useful imaging features. We can apply this effective, easy-to-use, non-invasive, complementary diagnostic tool in clinical practice. The nomogram will reduce the financial burden imposed on the health system and the psychological burden on patients. However, the performance of the model should be further investigated using a prospective dataset.

Funding This study has received funding from the science and technology project of Foshan (2017AB003623 and 2017AB003683).

Compliance with ethical standards

Guarantor The scientific guarantor of this publication is Qiugen Hu

Conflict of interest The authors of this manuscript declare no relationships with any companies, whose products or services may be related to the subject matter of the article.

Statistics and biometry No complex statistical methods were necessary for this paper.

Informed consent Written informed consent was waived by the Institutional Review Board.

Ethical approval Institutional Review Board approval was obtained.

Methodology
• retrospective
• diagnostic study
• performed at two institutions

References

1. Yoon JH, Lee HS, Kim EK, Moon HJ, Kwak JY (2016) Malignancy Risk Stratification of Thyroid Nodules: Comparison between the Thyroid Imaging Reporting and Data System and the 2014 American Thyroid Association Management Guidelines. Radiology 278(3):917–924
2. Gharib H, Papini E, Paschke R et al (2010) American Association of Clinical Endocrinologists, Associazione Medici Endocrinologi, and European Thyroid Association Medical Guidelines for Clinical Practice for the Diagnosis and Management of Thyroid Nodules. Endocr Pract 16(3):468–475
3. Xing M (2016) Clinical utility of RAS mutations in thyroid cancer: a blurred picture now emerging clearer. BMC Med 14:12
4. Burman KD, Wartofsky L (2015) CLINICAL PRACTICE. Thyroid Nodules. N Engl J Med 373(24):2347–2356
5. Haugen BR, Alexander EK, Bible KC et al (2016) 2015 American Thyroid Association Management Guidelines for Adult Patients with Thyroid Nodules and Differentiated Thyroid Cancer: The American Thyroid Association Guidelines Task Force on Thyroid Nodules and Differentiated Thyroid Cancer. Thyroid 26(1):1–133
6. Kim D, Kim DW, Heo YJ et al (2017) Computed Tomography Features of Benign and Malignant Calcified Thyroid Nodules: A Single-Center Study. J Comput Assist Tomogr 41(6):937–940
7. Shi RY, Yao QY, Zhou QY et al (2017) Preliminary study of diffusion kurtosis imaging in thyroid nodules and its histopathologic correlation. Eur Radiol 27(11):4710–4720
8. Pathak KA, Goertzen AL, Nason RW, Klonisch T, Leslie WD (2016) A prospective cohort study to assess the role of FDG-PET in differentiating benign and malignant follicular neoplasms. Ann Med Surg (Lond) 12:27–31
9. Raue F, Frank-Raue K (2016) Thyroid Cancer: Risk-Stratified Management and Individualized Therapy. Clin Cancer Res 22(10):5012–5021
10. Kaur K, Sonkhya N, Bapna AS, Mital P (2002) A comparative study of fine needle aspiration cytology, ultrasonography and radionuclide scan in the management of solitary thyroid nodule: A prospective analysis of fifty cases. Indian J Otolaryngol Head Neck Surg 54(2):96–101
11. Tae HJ, Lim DJ, Baek KH et al (2007) Diagnostic value of ultrasonography to distinguish between benign and malignant lesions in the management of thyroid nodules. Thyroid 17(5):461–466
12. Oberije C, Nalbantov G, Dekker A et al (2014) A prospective study comparing the predictions of doctors versus models for treatment outcome of lung cancer patients: a step toward individualized care and shared decision making. Radiother Oncol 112(1):37–43
13. Iasonos A, Schrag D, Raj GV, Panageas KS (2008) How to build and interpret a nomogram for cancer prognosis. J Clin Oncol 26: 1364–1370
14. Abu-Rustum NR, Zhou Q, Gomez JD et al (2010) A nomogram for predicting overall survival of women with endometrial cancer following primary therapy: toward improving individualized cancer care. Gynecol Oncol 116:399–403
15. Sternberg CN (2006) Are nomograms better than currently available stage groupings for bladder cancer? J Clin Oncol 24:3819–3820
16. Kumamaru KK, Saboo SS, Aghayev A et al (2016) CT pulmonary angiography-based scoring system to predict the prognosis of acute pulmonary embolism. J Cardiovasc Comput Tomogr 10(6):473–479
17. Vasquez MM, Hu C, Roe DJ, Chen Z, Halonen M, Guerra S (2016) Least absolute shrinkage and selection operator type methods for the identification of serum biomarkers of overweight and obesity: simulation and application. BMC Med Res Methodol 16(1):154
18. Werga P, Wallin G, Skoog L, Hamberger B (2000) Expanding role of fine-needle aspiration cytology in thyroid diagnosis and management. World J Surg 24:907–912
19. Theoharis CG, Schofield KM, Hammers L, Udelsman R, Chhieng DC (2009) The Bethesda thyroid fine-needle aspiration classification system: year 1 at an academic institution. Thyroid 19(11): 1215–1223
20. Mathur A, Weng J, Moses W et al (2010) A prospective study evaluating the accuracy of using combined clinical factors and candidate diagnostic markers to refine the accuracy of thyroid fine needle aspiration biopsy. Surgery 148(6):1170–1176
21. Zhang F, Zhao X, Han R, Du M, Li P, Ji X (2017) Comparison of Acoustic Radiation Force Impulse Imaging and Strain Elastography in Differentiating Malignant From Benign Thyroid Nodules. J Ultrasound Med 36(12):2533–2543
22. Chandramohan A, Therese M, Abhraham D, Paul TV, Mazhuvanchary PJ (2017) Can ARFI elastography be used to differentiate parathyroid from thyroid lesions? J Endocrinol Invest 41(1):111–119

23. Zhan J, Diao XH, Chen L, Jin JM, Chen Y (2017) Role of Contrast-Enhanced Ultrasound in Diagnosis of Thyroid Nodules in Acoustic Radiation Force Impulse "Gray Zone". Ultrasound Med Biol 43(6): 1179–1186
24. Colakoglu B, Yildirim D, Alis D et al (2016) Elastography in Distinguishing Benign from Malignant Thyroid Nodules. J Clin Imaging Sci 6:51
25. Zahir ST, Vakili M, Ghaneei A, Sharahjin NS, Heidari F (2016) Ultrasound Assistance In Differentiating Malignant Thyroid Nodules From Benign Ones. J Ayub Med Coll Abbottabad 28(4): 644–649
26. Iqbal M, Mehmood Z, Rasul S, Inamullah H, Shah SS, Bokhari I (2010) Carcinoma thyroid in multi and uninodular goiter. J Coll Physicians Surg Pak 20(5):310–312
27. Chammas MC, de Araujo Filho VJ, Moysés RA et al (2008) Predictive value for malignancy in the finding of microcalcifications on ultrasonography of thyroid nodules. Head Neck 30(9):1206–1210
28. Rahimi M, Farshchian N, Rezaee E, Shahebrahimi K, Madani H (2013) To differentiate benign from malignant thyroid nodule comparison of sonography with FNAC findings. Pak J Med Sci 29(1):77–80
29. Kim EK, Park CS, Chung WY et al (2002) New sonographic criteria for recommending fine-needle aspiration biopsy of nonpalpable solid nodules of the thyroid. AJR Am J Roentgenol 178:687–691
30. Nikiforov YE, Seethala RR, Tallini G et al (2016) Nomenclature Revision for Encapsulated Follicular Variant of Papillary Thyroid Carcinoma: A Paradigm Shift to Reduce Overtreatment of Indolent Tumors. JAMA Oncol 2(8):1023–1029